Preprints of the 21st IFAC World Congress (Virtual)
Berlin, Germany, July 12-17, 2020

Automated Maneuvering in Confined Waters using Parameter Space Model and Model-based Control*

Martin Kurowski * **Agnes Schubert** ** **Torsten Jeinsch** *

* *University of Rostock, Germany*
(e-mail: martin.kurowski@uni-rostock.de).
** *University of Applied Sciences Wismar, Germany*
(e-mail: agnes.schubert@hs-wismar.de)

Abstract: The paper discusses methods to increase the level of automation in ship handling towards a possible autonomous operation. The focus is on maneuvering situations in confined waters within the velocity range between dynamic positioning and transiting. While performant automation solutions exist for specialized vessels, standard ships are operated manually in maneuvering situations. In this context, one challenge is to adapt a model for controller design of maneuvering vessels. It is a cumbersome task to parameterize the common hydrodynamical oriented models, especially for maneuvering standard ships. Therefore, a more experimental approach has been chosen to decrease the complexity of the model structure. In that way, the applied motion model is highly abstracted and has a minimal number of parameters which are mapped in parameter spaces. For motion control, a cascaded structure integrating a velocity and a maneuver control system has been designed. The low-level part consists of a model-based feedforward control applying the parameter space model implicitly. Further a simple decentralized multi-variable feedback controller is used. Here, a robust approach has been applied for controller parameterization by assigning a specific parameter space to each defined operation range. The methods are verified and validated with two demonstrators. Firstly a passenger vessel is used in a ship handling simulator and secondly real world experiments are performed applying an unmanned surface vehicle. The objective of these trials is automated maneuvering in the port of Rostock.

Keywords: Marine Systems, parameter space method, model-based control, robust control application, unmanned surface vehicle, simulation

1. INTRODUCTION

Ship traffic is growing worldwide because of progressing globalization. The result is a higher traffic volume in harbors and waterways with equivalent higher coordination effort. Additionally, the technological progress in the shipbuilding industry causes increasing size of vessels and operative changes such as fairway and passing limitations. Fig. 1 illustrates a typical maneuvering situation in the port of Rostock. Despite the obvious limitation of the maneuvering space, the risk of collisions or other dangerous situations is low if critical constellations, such as significant disturbances by wind, current, fog or errors in essential subsystems, are absent. However, statistics show that the number of accidents have been risen over the past years and therewith the costs within the shipping industry. Fields (2012) stated that the largest percentage of accidents (75−96%) was due to human failure or missing assistance systems. This is one of the reasons why efforts are being made to increase the level of automation in ship handling, especially in maneuvering situations as discussed in Schubert et al. (2019).

Fig. 1. Typical maneuvering situation of ships in the port of Rostock

In order to achieve a high automation level of ship operations, maneuvering of ships in confined waters is one key factor. Hence, academic and industrial partners started the joint project *GALILEOnautic* to develop modules for guidance, navigation and control systems for fully automated vessels cooperating with each other in areas with high safety and efficiency requirements, such as ports or narrow waterways. Therefore, the vessels motion control

* The work was funded by the German Federal Ministry of Economics and Technology (BMWi) and supported by the DLR Space Administration under the registration numbers 50NA1612 and 50NA1809.

system should ensure a safe automatic and closed-loop control of the vessels in different operation modes. Hence, a key challenge is to increase the automation level at low as well as negative ship velocities and in confined waters in order to enable automatic maneuvering.

2. PROBLEM FORMULATION AND RELATED WORK

Basis for further automation is the common guidance, navigation and control (GNC) structure. GNC systems work like a closed control loop at the highest hierarchical level, where navigation provides optimal solution for vehicle position, velocities and attitude calculated from equipped sensors, guidance generates the command values for the motion control system and control summarizes the modules for automatic motion control, with the aim to calculate the necessary control forces and torques generated by the propulsion and steering gears of the specific vehicle.

In general, there are two classes of ship GNC systems, which were developed simultaneously. On the one hand, there are the complex systems for dynamic positioning (DP) with components defined by IMO (1994), and on the other hand, the classical systems for heading control and path following applied to ferries, cargo or cruise vessels defined by CENELEC (2014). The two systems differ substantially in the working mode, respectively, the velocity range and the implemented methods. From the control-technological point of view, it is distinguished between disturbance attenuation during dynamic positioning using highly dynamic propulsion systems as a substantial technical requirement. In contrast, track control systems, discussed in Berking and Huth (2016), work as follow-up controllers at cruising speed using conventional propeller-rudder combinations with classic transport vessels. In technological applications, Breivik et al. (2015) give an overview about DP where linear control methods are used based on LQG designs. For transiting Berking and Huth (2016) describe cascaded designs using classical control approaches. What they have in common is that they are always designed for a restricted working range, for cruising speed or dynamic positioning.

For this reason, attempts were made to switch to a more experimental modeling for special vehicles. Eriksen and Breivik (2017) show this with the example of a high speed vehicle, which is in displacement and gliding mode. The acting forces and torques are difficult to describe, so that abstracting polynomials were used to model the speed over ground and the rotation around the vertical axis. In comparison, this paper examines the further abstraction and generalization of hydrodynamic influences and the application to maneuvering ships.

3. MODEL BACKGROUND

3.1 Equations of motion

The motion of marine vehicles is described in two reference systems. The movement on the Earth's surface is given in an Earth-fixed frame, which is defined as inertial North-East-Down frame. Additionally, a body-fixed frame is defined, which is fixed to the vehicle. The focus on surface vehicles reduces the degrees of freedom to the motion on the nearly undisturbed water surface. Basic notations are

- $\mathbf{x} = [u\ v\ r]^T$ as state vector containing the linear velocities surge (x-axis) and sway (y-axis) as well as the angular velocity yaw (around z-axis) in the body-fixed frame and
- $\mathbf{x}_e = [x_e\ y_e\ \psi]^T$ as vector of position and heading of the vehicle according to the Earth-fixed frame.

The dynamics of marine vehicles are described using the equations of motion

$$\dot{\mathbf{x}}_e = \mathbf{T}_b^e(\psi)\mathbf{x} \tag{1}$$

$$\mathbf{M}_h\dot{\mathbf{x}} + \mathbf{C}_h(\mathbf{x})\mathbf{x} = \mathbf{D}_h(\mathbf{x})\mathbf{x} + \mathbf{H}_a + \mathbf{H}_d, \tag{2}$$

where $\mathbf{M}_h$ describes the hydrodynamic inertia matrix which consists of the vehicle mass and moment of inertia including added inertia effects. $\mathbf{C}_h$ is the Coriolis and Centripetal matrix including added inertia effects. On the right-hand side, the sum of external forces and moments acting on the vehicle considers damping $\mathbf{D}_h(\mathbf{x})$, actuators $\mathbf{H}_a$ and disturbances $\mathbf{H}_d$ such as wind and current. Due to the considered application, wave loads and resulting roll and pitch motions as well as stiffness effects are neglected.

Nevertheless, parameterization of a closed physically oriented model described by Eq. (2) is extremely sophisticated, especially in maneuvering situation with low or negative velocities. Highly nonlinear hydrodynamic effects have to be considered and determined by extensive towing tests in shipbuilding research institutes with functional models. In open sea trials, it is a cumbersome task to identify the unknown parameters of the nonlinear model due to strong couplings of the motion variables, measurement noise and unknown disturbances.

3.2 Parameter space model

For model-based control in combination with robust controller parameterization, the choice of vehicle model is a matter of the utmost importance. This choice is mostly motivated by the types of vehicles considered and their range of motions. In order to overcome the disadvantages of parameterizing the common model structure studied so far, further model simplification has been made to handle parameter uncertainties in the robust controller design.

Basis of the parameter space model are the equations of motion given with Eq. (2). The forces and torques of the propulsion and steering devices are not exclusively described as efficiencies in the respective primary direction. Rather, resistance-increasing force components and cross-couplings, such as those of a rudder or a turned propeller, are taken into account and influence the respective transition parameters. In other words, an abstraction of the different physical effects takes place to a combined effect on the motion degrees of freedom of the vehicle.

Finally, the physical description should be abstracted to apply a straightforward connection between the system inputs and outputs. In that way, existing cross-couplings between the internal states and the manipulated variables are added to the sum of external forces and torques. The interacting forces and torques of the actuators and the disturbances generate a predictable stationary value of the respective state variable. This stationary value is

indirectly influenced by the cross-couplings and changes with the motion states. The abstraction is achieved by linearizing the reduced equation of motion around $\mathbf{x}_0 = [u_0\ v_0\ r_0]^T$ which results in the description of the transition behavior between equilibrium points of the vehicle motion. A number of those linearizations leads to the parameter variable form

$$\mathbf{M}_h\dot{\mathbf{x}} = \mathbf{D}_G(\mathbf{x}_0, \Delta\mathbf{H}_G)\mathbf{x} + \mathbf{H}_a + \mathbf{H}_d \tag{3}$$

for a set of working points in the operating range of the vehicle. The resulting generalized damping parameter describes the specific dynamic behavior as a function of the actual states $\mathbf{x}_0$ and the differential forces and torques $\Delta\mathbf{H}_G = \Delta\mathbf{H}_a + \Delta\mathbf{H}_d$. After rearrangement, Eq. (3) can be rewritten as a parameter variable state space model

$$\dot{\mathbf{x}} = \mathbf{A}\mathbf{x} + \mathbf{M}_h^{-1}\mathbf{H}_a + \mathbf{M}_h^{-1}\mathbf{H}_d, \tag{4}$$

defining the system matrix

$$\mathbf{A} = \mathbf{M}_h^{-1}\mathbf{D}_G = \begin{bmatrix} f_{X_D}(.) & 0 & 0 \\ 0 & f_{Y_D}(.) & 0 \\ 0 & 0 & f_{N_D}(.) \end{bmatrix} \tag{5}$$

as functions of the states in the operating point $\mathbf{x}_0$ and the differential forces and torque exerting the system $\Delta\mathbf{H}_G$. The parameters are saved in characteristic maps defining $f_{X_D} = m_x^{-1}X_D$, $f_{Y_D} = m_y^{-1}Y_D$ and $f_{N_D} = J_z^{-1}N_D$.

The connection of the virtual actuator forces and torques $\mathbf{H}_a$ with the specific actuators of the vehicle $\mathbf{u}$ as well as the influence of the disturbances $\mathbf{H}_d$ results from similarly generated descriptions. An example of the resulting actuator standardization $\mathbf{A}_S$ can be given by

$$\mathbf{H}_a = \mathbf{A}_S\mathbf{u} = \begin{bmatrix} f_{X_{EOT}}(.) & f_{X_\delta}(.) & f_{X_{T_B}}(.) \\ 0 & f_{Y_\delta}(.) & f_{Y_{T_B}}(.) \\ 0 & f_{N_\delta}(.) & f_{N_{T_B}}(.) \end{bmatrix} \begin{bmatrix} EOT \\ \delta \\ T_B \end{bmatrix} \tag{6}$$

as the characteristic maps for a standard ship with engine-order-telegraph of a fixed propeller EOT, rudder δ and bow-thruster T_B.

Furthermore, for the stationary velocity components of a maneuver sequence can be estimated by

$$\hat{\mathbf{x}}_\infty = \begin{bmatrix} \hat{u}_\infty \\ \hat{v}_\infty \\ \hat{r}_\infty \end{bmatrix} = \begin{bmatrix} f_u(X_G, \mathbf{x}_0) \\ f_v(Y_G, \mathbf{x}_0) \\ f_r(N_G, \mathbf{x}_0) \end{bmatrix} \tag{7}$$

considering $\mathbf{x}_0$ as well as the summation of absolute forces and torques from actuator standardization and prevailing disturbances $\mathbf{H}_G$.

In contrast to a closed physical description of the hydrodynamic influences, the proposed model focuses on the strong abstraction of maneuvering behavior to reduce the number of necessary parameters to a minimum. In order to achieve an appropriate model quality, the complexity of the regarded parameters is increased. Due to the generalized form, it can be adapted to different vehicle classes without taking into account individual parameters of special types. The parameter values are stored in characteristic maps. This is also a disadvantage of the abstracted model approach. A large number of comparatively simple maneuvers is required to determine the corresponding parameters for the static and dynamic part of the parameter space model as will be shown in section 5.2. Since nonlinear motion behavior is mapped using linearized partial models, deviations occur, which inevitably increase with rising difference to the corresponding equilibrium point. However, it is assumed that the controlled process operates within the limits, where the simplified model provides a proper representation of dynamic behavior.

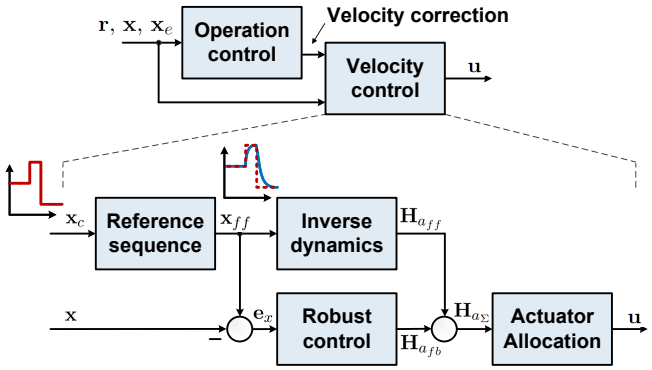

Fig. 2. Cascaded control structure regarding the components feedforward and feedback control, allocation and superior control in the specific operating range

4. CONTROL

4.1 Control structure

The local vehicle control system has to integrate different operation modes of the specific vessel. This includes independent vehicle control for transit and maneuvering or dynamic positioning for common and specialized ships. In addition, as described in this paper, the control system is to be used to allow automatic maneuvering operations. Therefore, a cascaded control structure has been considered using a unified inner loop and a variable outer loop, as introduced for USVs in Kurowski et al. (2015). The inner loop is designed as vehicle-specific multiple-input-multiple-output velocity control system which is fed by the outer operation loop. It is obvious that the different parts of the control system have to be adapted to the various operation modes, e.g. using switched structures. Fig. 2 illustrates the modular structure of the control system. The discussion about the model-based implementation of the different modules is given in the following sections.

Essential part of this structure is the velocity control system which corresponds to the vehicle-specific cascade and manipulates the available actuators in order to realize the desired transverse and rotational components. In order to achieve automated maneuvering capabilities, a two degrees of freedom controller is provided to separate the reference following behavior from damping of disturbances and achieving robustness. The velocity control system combines the functional main components model-based feedforward, robust feedback and actuator allocation, what is essential for maneuvering vehicles utilizing different actuator configurations.

4.2 Model-based feedforward

The model-based feedforward control should ensure that the vector of the controlled variables $\mathbf{y} = \mathbf{C}\mathbf{x}$ equals the feedforward states $\mathbf{x}_{ff}$ according to $\mathbf{x}_{ff} \overset{!}{=} \mathbf{x} = \mathbf{y}$. $\mathbf{C} = \mathbf{I}$ is used for fully actuated vehicles. Taking into account the system properties, rearranging Eq. (3) leads to the forces and moments of the feedforward control

$$\mathbf{H}_{a_{ff}} = \mathbf{M}_h\dot{\mathbf{x}}_{ff} - \mathbf{D}_G\mathbf{x}_{ff} \tag{8}$$

as a function of the feedforward states and neglecting disturbances $\mathbf{H}_d = \mathbf{0}$.

The system parameters $\mathbf{D}_G$ and $\mathbf{M}_h$ are applied on the basis of the current maneuver point using the available parameter tables. For this purpose, the static final value of the forces and moments is decoupled from the inverse dynamics and Eq. (8) can be changed to

$$-\mathbf{D}_G^{-1}\mathbf{H}_{a_{ff}} = -\mathbf{D}_G^{-1}\mathbf{M}_h\dot{\mathbf{x}}_{ff} + \mathbf{x}_{ff}. \tag{9}$$

It is obvious that the expression $-\mathbf{D}_G^{-1}\mathbf{H}_{a_{ff}}$ on the left side of Eq. (9) is a velocity vector. Taking into account the equilibrium of forces and torque in stationary case, the expression corresponds to the estimated velocities defining $-\mathbf{D}_G^{-1}\mathbf{H}_{a_{ff}} = \hat{\mathbf{x}}_\infty$. Consequently, the inverse dynamics of the model-based part of the feedforward control can be summarized as

$$\hat{\mathbf{x}}_\infty = -\mathbf{D}_G^{-1}\mathbf{M}_h\dot{\mathbf{x}}_{ff} + \mathbf{x}_{ff}. \tag{10}$$

By definition, the parameters $\mathbf{D}_G^{-1}\mathbf{M}_h$ are the inverse entries of the system elements from Eq. (5) which can be obtained directly from the characteristic maps using

$$\mathbf{D}_G^{-1}\mathbf{M}_h = \begin{bmatrix} f_{X_D}(\Delta X_{a_c}, \mathbf{x}_0)^{-1} & 0 & 0 \\ 0 & f_{Y_D}(\Delta Y_{a_c}, \mathbf{x}_0)^{-1} & 0 \\ 0 & 0 & f_{N_D}(\Delta N_{a_c}, \mathbf{x}_0)^{-1} \end{bmatrix}. \tag{11}$$

The components of vector $\Delta\mathbf{H}_{a_c} = [\Delta X_{a_c}\ \Delta Y_{a_c}\ \Delta N_{a_c}]^T$ required as inputs of the characteristic maps describe the differential forces and torque differences necessary to reach new reference values given by $\mathbf{x}_c$. The differences are calculated using the absolute forces and torque $\mathbf{H}_{a_c}$ required for the commanded state vector $\mathbf{x}_c$ and the absolute forces and torque $\mathbf{H}_a$ at the actual operating point $\mathbf{x}_0$.

Finally, the inverted entries of the characteristic maps given by Eq. (7) are used to calculate the absolute forces and torque of the feedforward control considering

$$\mathbf{H}_{a_{ff}} = \begin{bmatrix} X_{a_{ff}} \\ Y_{a_{ff}} \\ N_{a_{ff}} \end{bmatrix} = \begin{bmatrix} f_u(\hat{u}_\infty, \mathbf{x}_0)^{-1} \\ f_v(\hat{v}_\infty, \mathbf{x}_0)^{-1} \\ f_r(\hat{r}_\infty, \mathbf{x}_0)^{-1} \end{bmatrix}. \tag{12}$$

Due to the inversion, the input signal has to be differentiated. For physical realization of the feedforward terms the reference sequence adapts the commands $\mathbf{x}_c$ for feeding the inversion-based dynamics module using linear model-based filter structures. In principle, the order of this reference filters corresponds to the vector rank of the considered process model. Hence, the reference sequences for each degree of freedom can be defined as transfer functions

$$\mathbf{G}_{ref}(s) = \mathrm{diag}\{X_{ref}(s), Y_{ref}(s), N_{ref}(s)\}. \tag{13}$$

For the model-based approach, the dynamics of the vehicle already considered in the feedforward part are used similarly. Taking into account the vector degree the filter can be defined as

$$\mathbf{p}_{ref}\dot{\mathbf{x}}_{ff} + \mathbf{x}_{ff} = \mathbf{x}_c \tag{14}$$

where $\mathbf{p}_{ref} = \mathrm{diag}\{r_{u_1}, r_{v_1}, r_{r_1}\}$ are the design parameters. Likewise, these can be calculated directly from the characteristic maps of the model parameters according to

$$\begin{aligned} r_{u_1} &= -f_{X_D}(\Delta X_{a_{ref}}, \mathbf{x}_0)^{-1} \\ r_{v_1} &= -f_{Y_D}(\Delta Y_{a_{ref}}, \mathbf{x}_0)^{-1} \\ r_{r_1} &= -f_{N_D}(\Delta N_{a_{ref}}, \mathbf{x}_0)^{-1} \end{aligned} \tag{15}$$

where $\Delta\mathbf{H}_{a_{ref}} = [\Delta X_{a_{ref}}\ \Delta Y_{a_{ref}}\ \Delta N_{a_{ref}}]^T$ is used to allow increased manipulated values. In practice, the limitations of the actuators have to be taken into account by extracting the limits in the specific operating range from the actuator standardization given with Eq. (6). Hence, the method has advantages compared to conventional, empirical approaches. On the one hand, an analytical form of the characteristic maps is not necessary, which has advantages when parameterizing the maps. On the other hand, limitations of the forces and torques can be taken directly from the maps, so that the filters always generate feasible reference sequences. Hence, system restrictions are mapped directly.

4.3 Robust feedback

Due to the model-based feedforward, the vehicle motion should be equal to the reference motion $\mathbf{x}_c \overset{!}{=} \mathbf{x}$. Since disturbances are to be expected, a feedback controller is required. As design model for the robust controller parameterization, Eq. (2) has been adapted to the error description

$$\mathbf{M}_h\dot{\mathbf{e}}_x = \left(\mathbf{D}_h(\mathbf{x}) - \mathbf{C}_h(\mathbf{x})\right)\mathbf{e}_x + \mathbf{H}_d \tag{16}$$

defining $\mathbf{e}_x = \mathbf{x}_c - \mathbf{x}$. In addition to the environmental and system disturbances, deviations due to parameter uncertainty of the applied model have to be considered by the feedback controller. It can be shown that the different disturbance sources have similar impact on the motion behavior. Since constant or slowly varying disturbances are to be expected according to Eq. (16), integral behavior is required. Due to the methodology using the generalized controller design model a decentralized multi-variable controller has been designed for the considered degrees of freedom. As the parameters change during vessel maneuvering acording to the characteristic maps, the parameter space method is used for robust controller synthesis. In this context, spaces for different operation modes of the vessel are created in which specific parameters change. Hence, the design procedure should find a suitable controller candidate for the specific parameter space. The minimum and maximum values for the transition parameters are obtained from the corresponding characteristic maps of the parameter space model by inserting the range limits, e.g. $\min m_x^{-1}X_D = \min f_{X_D}(\Delta X_G, u_0)$ und $\max m_x^{-1}X_D = \max f_{X_D}(\Delta X_G, u_0)$.

Calculation of the controller parameters can be carried out using classical design methods, e.g. specifying the desired eigenvalues. Thus, the resulting controllers are generally less complex, but provide a robust parameterization. For the controllable degrees of freedom of the specific vessels discussed in this paper, PI structures are used on the velocity level. Since the vehicles have actuator limitations, anti-wind-up strategies have to be taken into account in the vehicle-specific structures.

Finally, the summation of feedforward and feedback leads to $\mathbf{H}_{a_\Sigma} = \mathbf{H}_{a_{ff}} + \mathbf{H}_{a_{fb}}$ to manipulate the vehicle motion. Due to the modular approach, the calculated forces and moments are separated from the current actuator configuration. Hence, the allocation module distributes them to the actuator arrangement of the specific vehicle.

5. EXPERIMENTAL RESULTS

5.1 Demonstrators

Firstly, as simulation environment a nautical ship handling simulator (SHS) ANS5000 from Rheinmetall Electronics GmbH is used. The simulator can be equipped with several ship bridges using original on-board equipment. Besides that further simulators can be operated integratively, e.g. ship engine or traffic simulator, see Benedict and Bornhorst (2010) for detailed information about the SHS. The implemented hydrodynamically oriented model takes into account effects such as moving at different water depths or in strongly changing depth profiles (banking) which influence the motion behavior of the vessel. Furthermore, characteristics of different actuators with regard to their physical limits as well as interactions between the drives are simulated. This is crucial in particular for the port maneuvers to be carried out.

Secondly, for real world tests the USV MESSIN is used as test vehicle to validate the developments during experimental trials. MESSIN is an agile catamaran with a length of 3.5 m, a breadth of 1.7 m and a displacement of 325 kg. The navigation sensors include an IMU based on optical gyros, a DGPS and a DVL. Propeller pods with an electrical power of 400 W are installed as propulsion units at the stern of the catamaran hulls, which realize a maximum vehicle speed of 4 kn. The podded drives are also used for steering, see Majohr and Buch (2006) for detailed information about the USV.

5.2 Modelling verification

An iterative procedure is applied to parameterize the parameter space model. For this purpose, operating points of the vehicle have to be defined. The absolute coefficients for nonlinear damping of the longitudinal motion and the components of nonlinear damping of the steering motion are then determined as a function of the operating points from run-out tests. In order to parameterize the actuator standardization according to example Eq. (6), simple maneuvering or step trials are performed, whereby the stationary values are evaluated. The characteristic maps of the estimated maneuver velocities according to Eq. (7) are generated using the data of the maneuvering trials and compared to the determined damping parameters. Finally, the values for the maneuvering dynamics according to Eq. (5) are identified using the maneuvers.

Verification of the method was carried out with the USV MESSIN. The two podded drives are controlled as a single unit. By turning the devices, additional transverse thrust and torque is generated in relation to the angle δ. The turning range is defined as $-45 \leq \delta \leq 45°$. Fig.,3 shows the resulting characteristic maps and additional parameters. In summary, it can be stated that plausible curves can be created even without further processing of the characteristic maps. This illustrates the robust character of the methods.

For model verification, simulations were compared with velocity data from tests with USV MESSIN. Fig. 4 shows the results of an arbitrary maneuver sequence using the podded drives in the entire operation range of $-100 \leq EOT \leq 100\%$ and $-45 \leq \delta \leq 45°$. As a result, the longitudinal velocity of the vehicle varies in almost the whole defined operation range from $0 < u < 2$ m/s, where the u and r are mapped well. The right part of the figure shows the change of the values of the parameter space model, whereby almost the entire range is covered due to the maneuvers.

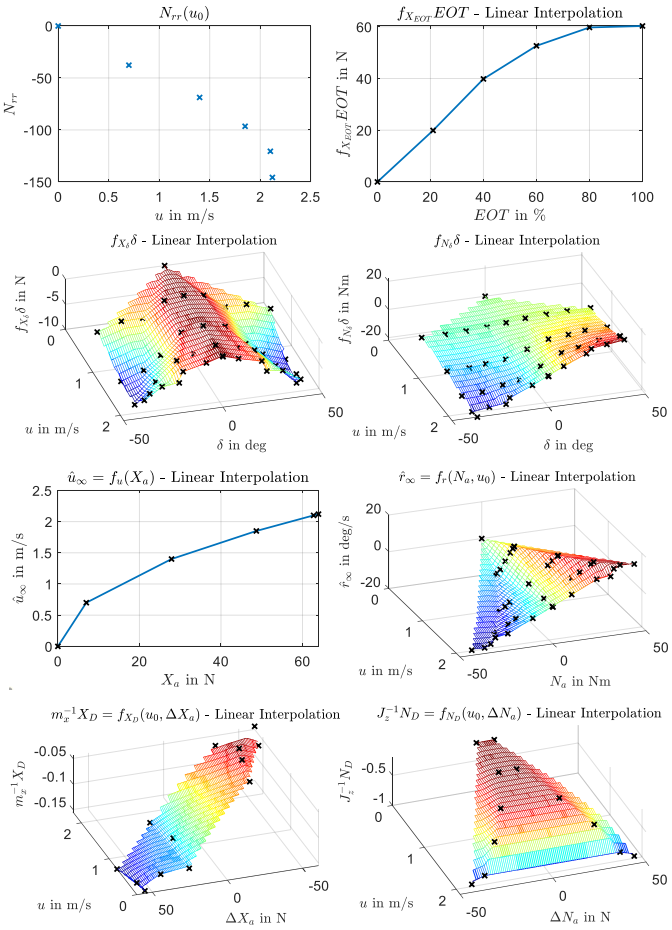

Fig. 3. Experimental parameterization of the parameter space model of USV MESSIN

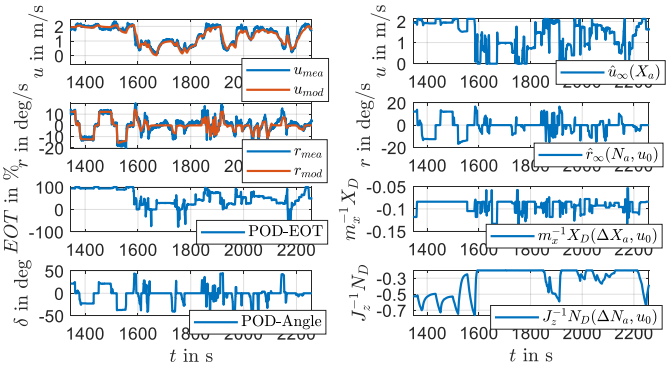

Fig. 4. Verification of the model approach using USV MESSIN showing the states (left) and the changing model parameters (right)

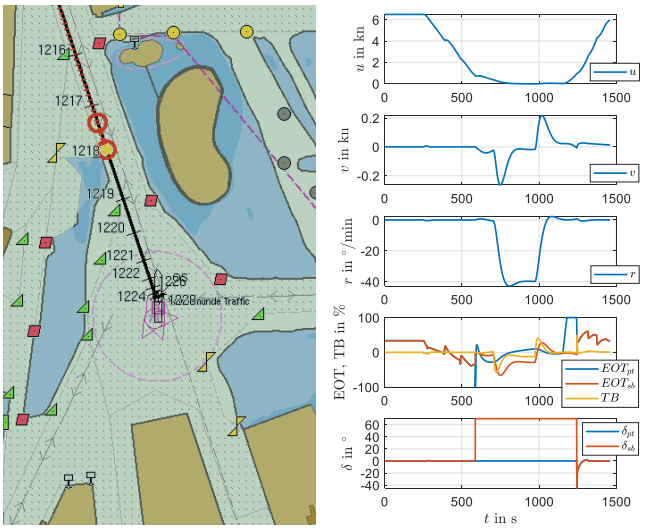

Fig. 5. Simulation of an automated turning maneuver in port of Rostock with the cruise ship MV Europa using model-based feedforward and robust feedback control

5.3 Maneuvering trials

The cruise ship MV Europa was used with the SHS to validate the automated maneuvering control operation. The vehicle is equipped with two podded drives and a bow transverse thruster. The manipulating values for the control system are the propulsion commands in EOT and turning angle δ as well as T_B for the bow thruster. The vessel has a length of about 200 m, a width of 24 m and a draught of 6 m. In order to be able to evaluate the performance of the control system while maneuvering, a turning maneuver on the turning plate in port of Rostock was chosen as simulation scenario. The command path was generated by choosing a manually driven maneuver. Fig. 5 shows the simulations results. The maneuver starts at the port entrance with a longitudinal velocity u of about 6.5 kn. After $t = 270$ s the ship starts to decelerate to about 0 kn while approaching the turning plate. During that deceleration the controller parameters change continuously due to the parameter space model as well as considering different actuator configurations and allocation constraints. During $590 < t < 1245$ s the vehicle turns with a yaw rate r of about $40°/min$ using the bow thruster and one of the podded drives which has been turned around 70° to allow to compensate the transversal velocity v. Hence, only small maneuvering space is used for the turning maneuver. Finally, the vehicle accelerates and moves to its berthing place. The maneuver cutout on the left side of the figure corresponds to the time $t = 1000$ s.

6. CONCLUSION

The paper showed methods for modelling and control for marine vehicles to realize accurate automated maneuvering with low vessel speed and high impact of the actuators. Therefore, an abstracted and simplified model based on characteristic maps has been created which can be used implicitly for model-based controller parameterization. Further, it was shown that a complete inversion of the characteristic maps is not necessary, which is advantageous with regard to the practical implementation and the robustness of the approach. The control system has been structured in a vehicle-specific and an operation-based loop. For verification of the methods different demonstrators have been applied using an USV in real world experiments and a cruise vessel in a ship handling simulator, what shows the robustness of the approach. For the next steps, the approach will be applied to the German research vessel DENEB and subsequently maneuvering tests will be carried out in the port of Rostock.

ACKNOWLEDGEMENTS

The authors would like to thank the German Federal Ministry for Economic Affairs and Energy (BMWi) and the DLR Space Administration for funding and supporting the project GALILEOnautic I + II under the registration numbers 50NA1612 and 50NA1809.

REFERENCES

Benedict, K. and Bornhorst, C. (2010). Maritime Simulation Technology for Training and Research at the Maritime Simulation Centre Warnemünde MSCW. In *Proceedings of the 8th IFAC Conference on Control Applications for Marine Systems*, 126–131. Rostock, Germany.

Berking, B. and Huth, W. (eds.) (2016). *Handbuch Nautik - Navigatorische Schiffsführung, 2. Auflage*. DVV Media Group, Seehafen Verlag, Hamburg.

Breivik, M., Kvaal, S., and Østby, P. (2015). From Eureka to K-Pos: Dynamic Positioning as a Highly Successful and Important Marine Control Technology. In *Proceedings of the 10th Conference on Manoeuvring and Control of Marine Craft*, 313–323. Copenhagen, Denmark.

CENELEC (2014). Maritime navigation and radiocommunication equipment and systems - Track control systems. European Standard EN 62065:2014, European Committee for Electrotechnical Standardization.

Eriksen, B.O. and Breivik, M. (2017). *Modeling, Identification and Control of High-Speed ASVs: Theory and Experiments*, 407–431. Springer International Publishing, Cham.

Fields, C. (2012). Safety and Shipping 1912-2012. Report, Allianz Global Corporate & Specialty.

IMO (1994). Guidelines for vessels with dynamic positioning systems. Technical Report MSC/Circ.645, International Maritime Organization.

Kurowski, M., Haghani, A., Koschorrek, P., and Jeinsch, T. (2015). Guidance, Navigation and Control of Unmanned Surface Vehicles. *at-Automatisierungstechnik, DeGruyter Oldenbourg*, 63(5), 355–367.

Majohr, J. and Buch, T. (2006). Modelling, simulation and control of an autonomous surface marine vehicle for surveying applications Measuring Dolphin MESSIN. In G. Roberts and R. Sutton (eds.), *Advances in Unmanned Marine Vehicles*, chapter 16, 329–352. The Institution of Electrical Engineers.

Schubert, A., Kurowski, M., Damerius, R., Fischer, S., Gluch, M., Baldauf, M., and Jeinsch, T. (2019). From Manoeuvre Assistance to Manoeuvre Automation. *Journal of Physics: Conference Series*, 1357, 012006. doi:10.1088/1742-6596/1357/1/012006.